Two interacting electrons in a vertical quantum dot with magnetic fields

J. T. Lin
National Center for Theoretical Sciences, Physics Division, P.O. Box 2-131, Hsinchu 30013, Taiwan and Department of Electronic Engineering, Chung Chou Institute of Technology, 6, Lane 2, Section 3, Sunchao Road, Yualin, Changhua 51042, Taiwan

T. F. Jiang
Institute of Physics, National Chiao Tung University, 1001 Ta-Hsueh Road, Hsinchu 30010, Taiwan
(Received 30 November 2000; revised manuscript received 19 July 2001; published 26 October 2001)

We present a numerical exact calculation for the energy spectra of two electrons in a finite height cylindrical quantum dot in details by a coupled-channel method. The electron correlation energy for various geometry of quantum dots, with and without applied magnetic fields, for singlet and triplet states are investigated. The magnitude of magnetic field for transition of the spin-singlet ground state and the spin-triplet excited state is compared with experimental result. The study shows significant contributions due to the spreading of electron density distribution along the vertical direction. In contrast to the planar circular disk model, the study will be useful for some realistic quantum dots.

DOI: 10.1103/PhysRevB.64.195323 PACS number(s): 73.21.−b, 71.45.Lr

I. INTRODUCTION

Two-electron quantum dot is the simplest quantum dot system that shows the interplay of electron-electron interaction and spin effects and hence is especially interesting. Without external magnetic field, spin singlet is the ground state and the degenerate spin triplet is the first excited state. With applied magnetic field, the triplet states split and shifted while the singlet state has zero spin and change slower in energy than one of the triplet states as magnetic field increases. At certain magnetic field strength, the triplet and singlet states interchange the roles of the ground and excited states. Similar oscillations occur at higher excited states, too. Unlike the situations of quantum dots, the singlet-triplet crossing for helium atom will be at magnetic field as high as 4×10^4 T and yet to be observed. Among the studies of two electrons in a quantum dot, Wagner *et al.*[1] derive the perturbation results for the spin singlet-triplet oscillations for two electrons in a circular disk model quantum dot under perpendicular magnetic field. The oscillation was observed by Ashoori *et al.*[2] The experiment which used vertical confined quantum dot (called the vertical quantum dot) was an $Al_{0.3}Ga_{0.7}As/GaAs$ quantum well of diameter 408 Å and height 175 Å with the parabolic lateral confined potential $\frac{1}{2}m^*\omega_\perp^2 r^2$ of $\hbar\omega_\perp=5.4$ meV. The measured cross-over occurs at about 1.5 T. By using a model of two-dimensional circular disk Wagner *et al.*[1] found the crossing at 3.6 T with their calculation.

Other physics of two electrons in semiconductor quantum dots has been intensively investigated in the past few years. Bryant[3] studied the energy levels for two electrons in a square GaAs quantum-well box. Merkt *et al.*[4] calculated two electrons states in semiconductor quantum dot with harmonic-oscillator well under perpendicular magnetic fields. Pfannkuche *et al.*[5] compared the results of Hartree, Hartree-Fock and exact treatment for the same system. They found that the Hartree-Fock is good for the triplet states but not appropriate for the singlet state, so the exchange and correlation effects are very important for few-electron quantum dots. Dineykhan and Nazmitdinov[6] used oscillator representation to study the two-electron quantum dots in magnetic fields. They found that the height of a quantum dot actually modifies the value of magnetic field for the observation of the singlet-triplet oscillation. While most of the studies are based upon model of planar disk, their study includes the vertical dimension.

The electron-electron interaction effects include the mutual Coulomb term and spin part. Experimentally, the FIR results[7] show that the parabolic confining potential is a good approximation. So the *N*-electron Hamiltonian in a quantum dot can then be separated as center-of-mass (c.m.) motion and relative motion (RM) due to the parabolic potentials. The FIR acts on c.m. only and the electron-electron effects are hard to detect. To explore the electron-electron interaction, Wagner *et al.*[1] proposed the measurements of magnetization or the spin singlet-triplet oscillations for the exploration of electron-electron interaction.

Due to the relative smallness of the height with respect to the diameter in a vertical quantum dot, most of the studies of this problem used the model of two-dimensional circular disk.[8] However, although the motion of electrons in *z* direction is mostly confined in the ground state subband, the distribution in *z* direction is very important for the dominant role of electron-electron Coulomb interaction. Rontani *et al.*[9] found that purely 2D models often inadequately describe the Coulomb interaction, and overestimate the carrier localization. Considering so many investigations of this problem with circular model, a more detailed calculation related to the realistic quantum dots is certainly demanding.[10] In this paper, we calculate the energy spectra of two interacting electrons in the vertical quantum dot under magnetic field by a coupled-channel method. The method is numerical exact for two-electron system under magnetic fields. In a recent paper, the method was employed to solve the additional energy spectra of many-electron system in vertical and spherical quantum dots.[11] We must point out that the method is

readily to be generalized for other types of potential; however, as shown in Ref. 10, the parabolic potential is accurate for radius less than 700 Å. Hence in this paper, we will limit our scope to the parabolic confining potentials.

II. THE EXACT TREATMENT OF TWO-ELECTRON VERTICAL QUANTUM DOT WITH PARABOLIC CONFINEMENT POTENTIALS

We consider two interacting electrons of effective mass m^* in a vertical quantum dot with harmonic confinement potential. In the presence of a constant magnetic field B in the z direction, the system is described by the Hamiltonian

$$H=\sum_{j=1}^{2}\left\{\frac{1}{2m^*}\left(\vec{\mathbf{p}}_j-\frac{e}{c}\vec{\mathbf{A}}_j\right)^2+V_{\rm dot}(\vec{\mathbf{r}}_j)\right\}+\frac{e^2}{\epsilon|\vec{\mathbf{r}}_1-\vec{\mathbf{r}}_2|}+H_{\rm spin}, \tag{1}$$

where the confinement potential $V_{\rm dot}(\vec{\mathbf{r}}_j)=(m^*/2)[\omega_\perp^2(x_j^2+y_j^2)+\omega_z^2 z_j^2]$ and $H_{\rm spin}=g^*\mu_B(\vec{\mathbf{s}}_1+\vec{\mathbf{s}}_2)\cdot\vec{\mathbf{B}}$ is the coupling of electron spin and magnetic field. μ_B is the Bohr magneton and the background dielectric constant is ϵ. The effective atomic units are used hereafter unless otherwise stated, that is $\hbar=m^*=e/\sqrt{\epsilon}=1$. For GaAs one has $\epsilon=12.4$ and $m^*=0.067$ which imply the effective Bohr radius $a_0^*=97.9$ Å and effective Hartree energy $E_0^*=11.9$ meV. The effective $g^*=0.44$ is from band parameters of GaAs.[1,12] For the perpendicular magnetic field, we choose a symmetric gauge described by the vector $\vec{\mathbf{A}}=\frac{1}{2}\vec{\mathbf{B}}\times\vec{\mathbf{r}}=\frac{1}{2}B(-y,x,0)$. Introducing the relative and center-of-mass coordinate $\vec{\mathbf{r}}=\vec{\mathbf{r}}_1-\vec{\mathbf{r}}_2$, $\vec{\mathbf{R}}=(\vec{\mathbf{r}}_1+\vec{\mathbf{r}}_2)/2$, the Hamiltonian, Eq. (1) can be decomposed into the center-of-mass(c.m.) and relative-motion (RM) terms as follows:

$$H=H_{\rm c.m.}+H_{\rm RM}+H_{\rm spin}, \tag{2}$$

$$H_{\rm c.m.}=-\frac{1}{4}\nabla_R^2+\Omega_{\rm eff}^2(X^2+Y^2)+\frac{1}{2}\omega_c L_Z+\omega_z^2 Z^2, \tag{3}$$

and

$$H_{\rm RM}=-\nabla_r^2+\frac{1}{4}\Omega_{\rm eff}^2(x^2+y^2)+\frac{1}{2}\omega_c l_z+\frac{1}{4}\omega_z^2 z^2+\frac{1}{r}, \tag{4}$$

where $\Omega_{\rm eff}=\sqrt{\omega_\perp^2+\omega_c^2/4}$, and $\omega_c=eB/m^*c$ is the cyclotron frequency.

To solve the eigenenergy of the two electrons system, we calculate the eigenenergies of c.m. and RM parts separately. At the first glance, the c.m wave function contains a planar harmonic oscillator with angular frequency $\Omega_{\rm eff}$ and a z-direction harmonic oscillator with frequency ω_z. Its eigenenergy can be written as

$$E_{\rm c.m.}=(2N+|M|+1)\Omega_{\rm eff}+\left(N_Z+\frac{1}{2}\right)\omega_z+\frac{1}{2}\omega_c M, \tag{5}$$

where $N=0,1,2,3,\ldots$, and $M=$ integer. On the other hand, due to the Coulomb interaction, the RM wave function cannot be solved analytically. We expand the RM wave function in spherical harmonics:

$$\Psi_{\rm RM}(r)=\sum_l\frac{\phi_{i\sigma,l}(r)}{r}Y_{lm}(\Omega), \tag{6}$$

the eigenvalue equation reduces to the following coupled-channel form:

$$\left[-\frac{d^2}{dr^2}+\frac{l(l+1)}{r^2}+\frac{1}{4}\Omega_{\rm eff}^2 r^2+\frac{1}{2}\omega_c m+\frac{1}{r}\right]\phi_{i\sigma,l}(r)\,\delta_{l'l}+\sum_l\frac{1}{4}\Delta\omega^2 r^2 A_l^{l'm}\phi_{i\sigma,l}(r)=\epsilon_{i\sigma}\phi_{i\sigma,l}(r)\,\delta_{l'l}, \tag{7}$$

with

$$A_l^{l'm}=\int Y_{l'm}^*(\Omega)\cos^2\theta Y_{lm}(\Omega)\,d\Omega, \tag{8}$$

and $\Delta\omega^2=\omega_z^2-\Omega_{\rm eff}^2$.

The total wave function $\Psi(1,2)$ contains the product of c.m., RM and spin parts. Ψ must be antisymmetric under the interchange of two electrons. The c.m. part has parity $(-1)^{M+N_z}$, with the condition $\omega_z\gg\omega_\perp$, the electrons will always be in the $N_z=0$ subband. The parity in Eq. (6) is equal to $(-1)^l$, thus the index l in Eq. (6) must be either odd or even. Also, since the z component of angular momentum is conserved, both the L_z of Eq. (3) and l_z of Eq. (4) are good operators. The magnetic quantum numbers M and m are fixed for each state. Since the magnetic quantum number m is a good quantum number for each orbital, the orbital and spin coupling do not need to be included in the diagonalization scheme. The coupled equations (7) are solved to machine accuracy by means of the generalized pseudospectral (GPS) method.[13,14] For the radial coordinate r, we first map the range $[0,\infty]$ or $[0,r_{\rm max}]$ into $[-1,1]$ by using

$$r=r(x)=L\frac{1+x}{1-x+\alpha}, \tag{9}$$

where $\alpha=2L/r_{\rm max}$ and L is the mapping parameter. The collocation points $\{x_k\}$ and the corresponding weights are determined through the Gauss-Legendre-Lobatto quadrature.[14] The method is especially accurate for Coulomb problems. As a typical example, in the calculation of $B=10$ T, 50 grid points in r and 18 partial waves were used. The diagonalization takes about 18 cpu seconds on a 600 MHz Pentium III PC.

III. RESULTS AND DISCUSSIONS

In Fig. 1, we plot the total energy of two noninteracting electrons without spin term at $\omega_\perp=0.5$. As for the confinement in vertical direction, Fig. 1(a) is for $\omega_z=0.5$, Fig. 1(b) is for $\omega_z=1.0$, and Fig. 1(c) is for $\omega_z=5.0$, respectively. The system is decomposed into Eq. (3), and Eq. (4) without the

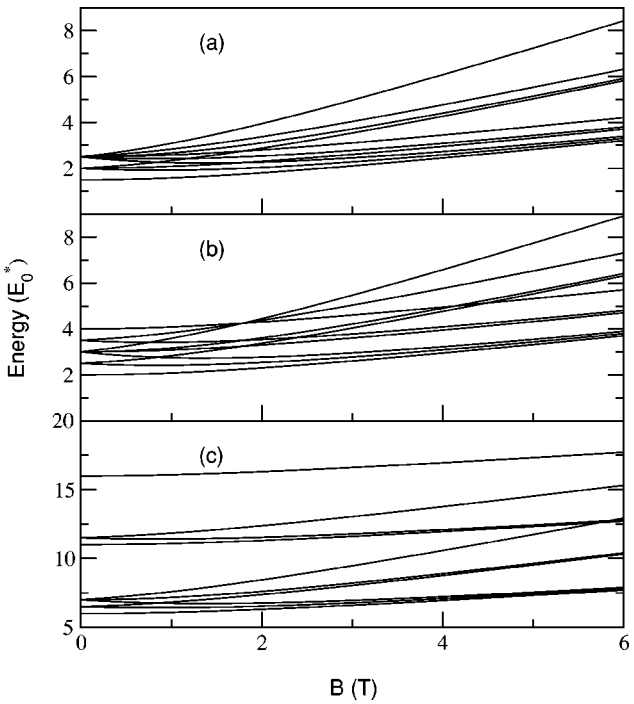

FIG. 1. Total energy of two noninteracting electrons in a quantum dot with $\omega_\perp = 0.5$ and different confinement ω_z in z direction under applied magnetic. For (a) $\omega_z = 0.5$, (b) $\omega_z = 1.0$, and (c) $\omega_z = 5.0$. The $\omega_\perp$ and ω_z are in *effective atomic unit* as described in the text.

Coulomb term. The total energy is equal to $E_{\text{c.m.}}$ of Eq. (5) plus

$$E_{\text{RM}} = (2n + |m| + 1)\Omega_{\text{eff}} + \left(n_z + \frac{1}{2}\right)\omega_z + \frac{1}{2}\omega_c m, \quad (10)$$

where $n = 0,1,2,3, \ldots,$ and $m =$ integer. By defining

$$\omega_\pm = \Omega_{\text{eff}} \pm \frac{1}{2}\omega_c, \quad (11)$$

$$N_\pm = N + \frac{1}{2}(|M| \pm M), \quad (12)$$

$$n_\pm = n + \frac{1}{2}(|m| \pm m), \quad (13)$$

we can see that the total energy is rewritten as

$$E_{\text{c.m.}} + E_{\text{RM}} = (N_+ + n_+ + 1)\omega_+ + (N_- + n_- + 1)\omega_- + (N_Z + n_z + 1)\omega_z. \quad (14)$$

In Landau regime $\omega_c \gg \omega_\perp$, the total energy becomes

$$E_{\text{c.m.}} + E_{\text{RM}} \rightarrow (N_+ + n_+ + 1)\omega_c + (N_Z + n_z + 1)\omega_z. \quad (15)$$

The energy levels we plot in Fig. 1 are designated by (N,M,N_Z,n,m,n_z). The orders from lower to higher levels near $B = 0$ are $(0,0,0,0,0,0)$, $(0,-1,0,0,0,0)$, $(0,0,1,0,0,0)$, $(0,1,0,0,0,0)$, $(0,-1,0,0,-1,0)$, $(0,-1,0,0,0,1)$, etc. in Fig. 1(a). Since $\omega_\perp = \omega_z = 0.5$, the confinement is a spherical harmonic oscillator potential and the quantum numbers of $E_{\text{c.m.}}$ and E_{RM} are of equal weight. For example, $(0,-1,0,0,0,0)$ and $(0,0,0,0,-1,0)$ are degenerate states so are the four states, $(0,-1,0,0,0,1),(0,-1,1,0,0,0),(0,0,0,0,-1,1)$ and $(0,0,1,0,-1,0)$. For small magnetic field B, those states with negative magnetic quantum number have lower energies due to azimuthal angular momentum coupling. And this coupling will eventually dominate the confinement potential for some states that makes the energy diagram more complicated for large B than small B's. In contrast to Fig. 1(a) which has three degenerate branches near $B = 0$, there are five degenerate branches near $B = 0$ in Fig. 1(b) because the confinement is not a spherical symmetric potential anymore. But the confinement ratio $\omega_z/\omega_\perp = 2$ is integer, the degeneracy of states still exists for $B \neq 0$. The energies from lower to higher near $B = 0$ in Fig. 1(b) are $(0,0,0,0,0,0)$, $(0,-1,0,0,0,0)$, $(0,1,0,0,0,0)$, $(0,-1,0,0,-1,0)$, $(0,0,1,0,0,0)$ and so on. Figure 1(c) indicates that there are 6 branches near $B = 0$ for $\omega_z = 5.0$ and the larger energy difference between these states at $B = 0$ compared to Figs. 1(a) and 1(b) is due to larger vertical confinement potential.

It is easy to deduce all the energies and their degeneracy in Fig. 1 from the exact form of Eq. (14). We plot this figure in order to show the effects of Coulomb and spin interactions in the next graph. Noted that under the parabolic potential forms, the lowest spin singlet and triplet energy will never cross each other, no matter how large the applied magnetic field is. This can easily be seen by the singlet and triplet energy from $E_{\text{c.m.}}$ and E_{RM}.

In Fig. 2, we show the difference of total energies of the calculation with and without both of the Coulomb and spin effects. The parameters of $\omega_\perp$ and ω_z are the same as those of Fig. 1. For simplicity, we present the energy difference of those low-lying states, that is, $N = 0$ and $n = 0$ in this figure. The states we draw from bottom to top in Fig. 2(a) are $S(0,0,-1,1)$, $T(-1,0,0,1)$, $T(0,0,-1,0)$ and $S(0,0,0,0)$ where $S(T)$ indicates the state is singlet(triplet) with quantum number (M,N_Z,m,n_z). There are many states which energy difference is the same curve in Fig. 2. The group, $S(0,0,-1,1)$ and $S(0,0,1,1)$, is represented by a curve and $S(0,0,0,0)$, $S(0,1,0,0)$, $S(1,0,0,0)$ and $S(-1,0,0,0)$ are in a group of the same curve. For triplet states, $T(0,0,-1,0)$ and $T(0,0,1,0)$ belong to a group and $T(-1,0,0,1)$, $T(0,0,0,1)$, $T(0,1,0,1)$ and $T(1,0,0,1)$ are in the same group. The difference in the singlet ground state is actually the dominant one among the few plotted low-lying states. This shows that the effects of electron correlation and exchange are more important for spin singlet ground state than for the triplet as shown in Ref. 5. Also noted that as the vertical confining potential changes, the behavior of these states also varies. The order of $T(-1,0,0,1)$ and $T(0,0,-1,0)$ merges into the same point at $B = 0$ for $\omega_z = 0.5$ and switches in the cases of $\omega_z = 1.0$ but not in the case of $\omega_z = 5.0$. This also means that the vertical confinement is physically significant to the behavior of electrons in a quantum dot.

To further explore the effect of vertical confinement on the energy spectra, we define the correlation energy as

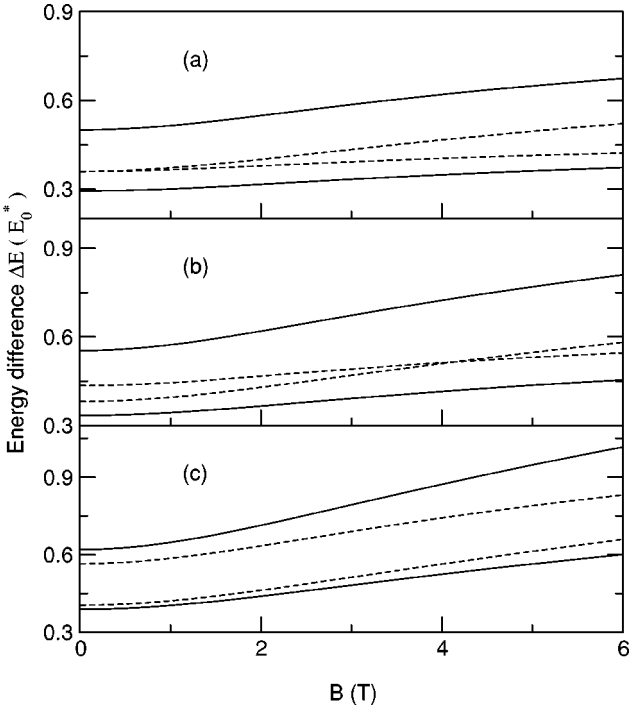

FIG. 2. The difference in total energy for the Hamiltonians with and without Coulomb interaction and spin effect. The shape of quantum dots studied corresponds to those of Fig. 1. Solid line is the energy difference of the singlet state and dashed line is for triplet state. The curves from bottom to top in energy at $B=0$ are $S(0,0,-1,1)$, $T(-1,0,0,1)$, $T(0,0,-1,0)$, and $S(0,0,0,0)$ in (a); the energy order in (b) is the same as (a) except that the triplet states exchange their order for large B value; in (c) the order is $S(0,0,-1,1)$, $T(0,0,-1,0)$, $T(-1,0,0,1)$, and $S(0,0,0,0)$. See text for the notation.

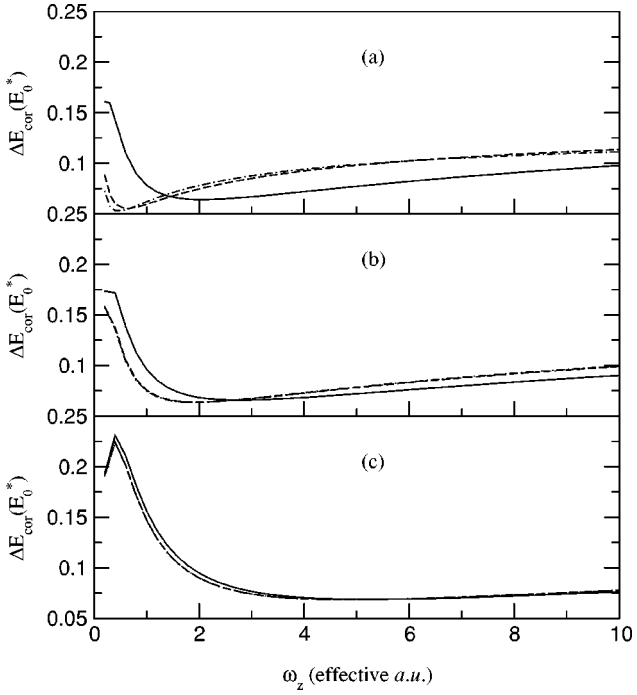

FIG. 3. The change of electron correlation energy with respect to the geometry of quantum dots under applied magnetic fields. The states are singlet states with $(n,m,n_z)=(0,0,0)$. In each plot, the solid line represents an applied field $B=10$ T, dashed line for $B=2$ T, and dotted-dashed line for $B=0$ T. (a) $\omega_\perp=0.5$, (b) $\omega_\perp=2$, and (c) $\omega_\perp=5$.

$$\Delta E_{\rm cor}=E_{\rm RM}-\left\{E^0_{\rm RM}+\left\langle\frac{1}{r}\right\rangle\right\}, \tag{16}$$

where the Hamiltonian of the relative motion in Eq. (4) is rewritten as

$$H_{\rm RM}=H^0_{\rm RM}+\frac{1}{r}, \tag{17}$$

and

$$H_{\rm RM}\Psi_{\rm RM}=E_{\rm RM}\Psi_{\rm RM}, \tag{18}$$

$$H^0_{\rm RM}\Psi^0_{\rm RM}=E^0_{\rm RM}\Psi^0_{\rm RM}, \tag{19}$$

$$\left\langle\frac{1}{r}\right\rangle=\left\langle\Psi_{\rm RM}\left|\frac{1}{r}\right|\Psi_{\rm RM}\right\rangle. \tag{20}$$

So $\Delta E_{\rm cor}$ is the difference of total energy in Eq. (18) from the energy of the noninteracting electrons in Eq. (19) and their direct Coulomb energy. In the regime of perturbation theory,

$$\Delta E_{\rm cor}=E_{\rm RM}-\left\langle\Psi^0_{\rm RM}\left|H^0_{\rm RM}+\frac{1}{r}\right|\Psi^0_{\rm RM}\right\rangle. \tag{21}$$

In Fig. 3 we show the change of correlation energy for the spin singlet state of $(n,m,n_z)=(0,0,0)$, with respect to the quantum dot geometry under magnetic fields of 0,2 T and 10 T. We plot the cases of $\omega_\perp=0.5,2$, and 5 with ω_z running from 0 to 10 at increment 0.2. We find that the correlation energy is larger for stronger magnetic field at small ω_z but reversed for larger ω_z, and the change of $\Delta E_{\rm cor}$ with respect to ω_z is smoother for larger values than at small values of ω_z.

The results can be explained as follows, since the motion of c.m. plays no role in the correlation, and only the part of relative motion is important. The correlation energy is proportional to the overlap of the electron wave functions. For the spin singlet state, we can estimate the wave function as

$$\Psi(r)\sim\exp\{-[\Omega_{\rm eff}(x^2+y^2)+\omega_z z^2]/4\}, \tag{22}$$

so the spatial spreading in horizontal dimension is $\sim 1/\sqrt{\Omega_{\rm eff}}$ and is $\sim 1/\sqrt{\omega_z}$ in the vertical direction. From the definition $\Omega_{\rm eff}=\sqrt{\omega_\perp^2+\omega_c^2/4}$, we can see that at small ω_z, the electrons become more and more localized in the horizontal direction as the magnetic field increases and hence the correlation energy will increase with the magnetic field. On the other hand, for the larger ω_z, the electron distribution in z direction is rather localized, the change of horizontal distribution due to the increase of magnetic field does not produce significant change in electron correlation.

In Fig. 4 we present the correlation energy with respect to the change of ω_z for more states. We calculated the singlet states with $(n,m,n_z)=(0,0,0),(0,1,1)$ and triplets with

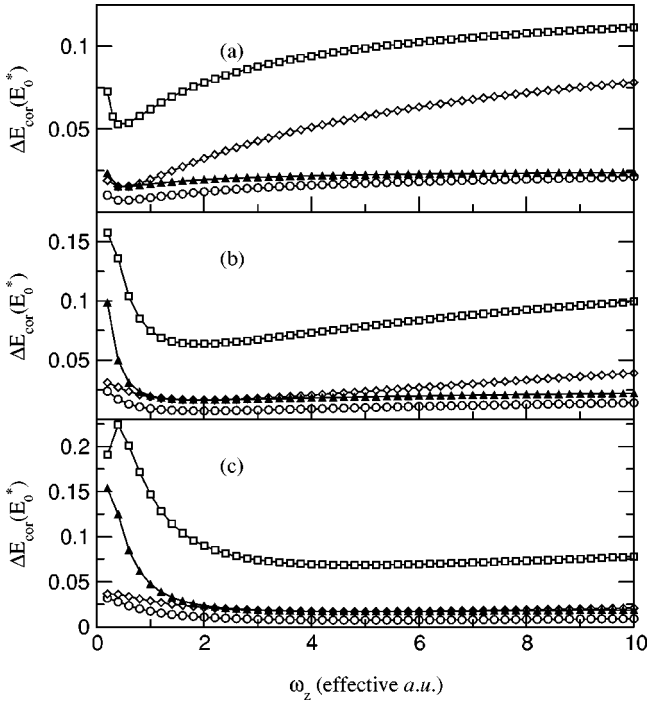

FIG. 4. The change of correlation energy for several states without magnetic field. In each plot, open-squared curve is for the singlet state with $(n,m,n_z)=(0,0,0)$, open circles for singlet with $(n,m,n_z)=(0,1,1)$, open diamonds for triplet with $(n,m,n_z)=(0,0,1)$, and filled upper triangles for triplet with $(n,m,n_z)=(0,1,0)$. (a) $\omega_\perp=0.5$, (b) $\omega_\perp=2$, and (c) $\omega_\perp=5$. Similar tendency is found for cases with $B=2$ T and $B=10$ T.

$(n,m,n_z)=(0,0,1)$ and $(0,1,0)$ at $B=0$. We can see that singlet state $(0,0,0)$ has the largest electron correlation and singlet state $(0,1,1)$ has the smallest correlation among the four curves. Again, this can be explained by the electron wave function overlap of the relative motion. The singlet $(0,1,1)$ have the most widely spreading density distribution and the smallest overlap to produce electron correlation. Similar tendency was found for the cases of $B=2$ T and $B=10$ T and is not shown.

To compare with the experimental data,[2] we use $\omega_\perp=5.4$ meV and $\omega_z=29.3$ meV to model the size ratio of diameter to height to be 408 Å:175 Å. We show in Fig. 5 the energy spectrum of two electrons in the vertical quantum dot under uniform magnetic field along the vertical direction. At smaller magnetic field, the spin singlet state is the ground state while the triplet states are the excited states. The $M=0$, $m=-1$ state of the triplet becomes the lowest one due to the magnetic filed at the value of $B=1.1$ T. Compared with the experimental $B=1.5$ T, the result is actually acceptable. Because this value of magnetic field depends on several physical parameters, such as the confinement potentials, the dielectric constants of material and size of the dot, etc. And the experimental conditions such as the confinement potentials and other material parameters are hardly the same as the idealized parameters employed in the calculation.

To further investigate the effects of potential parameters on the magnitude of the singlet-triplet transition magnetic field, we perform a calculation for a variety of quantum dot

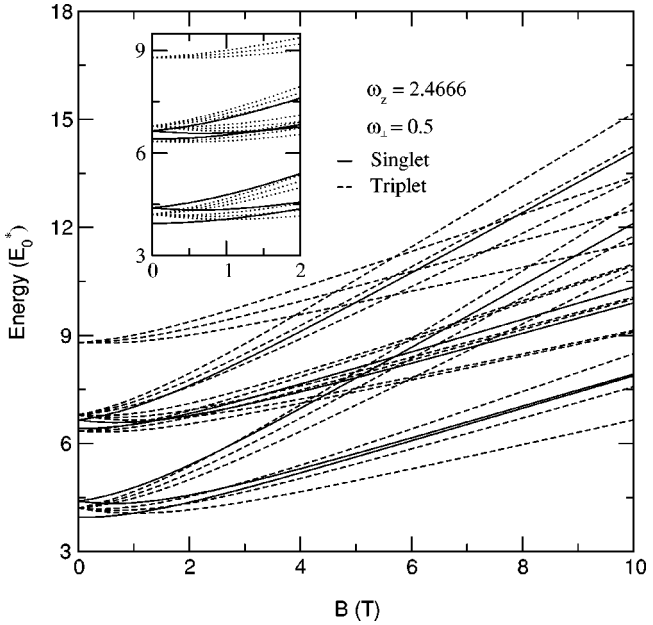

FIG. 5. Energy spectrum of two interacting electrons quantum dots. The confinement parameters are set to model the experiment with quantum dot of diameter 408 Å and height 175 Å. $\omega_z=2.4666$ corresponds to 29.3 meV.

geometry and size. In Fig. 6(a), we plot the transition magnetic fields against a range of ω_z at $\omega_\perp=0.454$ (i.e., 5.4 meV). This actually implies the change of the magnetic field with the geometry. At $\omega_z=\omega_\perp$, the quantum dot is

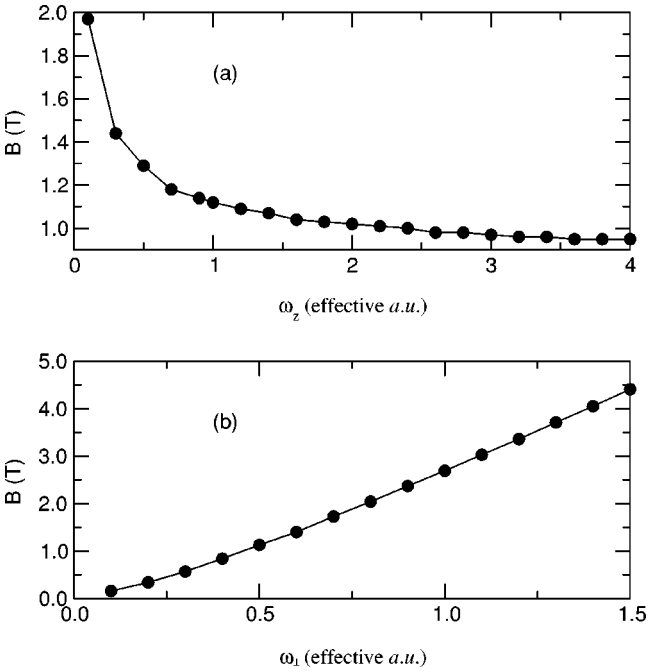

FIG. 6. The change of singlet-triplet crossover magnetic field with the geometry and size of the quantum dots. (a) For $\omega_\perp=0.454$: the dot is cigar shape for $\omega_z \ll \omega_\perp$, and is spherical for $\omega_z=\omega_\perp$. At $\omega_z \gg \omega_\perp$, the dot approaches planar disk. (b) For $\omega_z/\omega_\perp=5.436$: smaller $\omega_\perp$ corresponds to larger vertical dot, and vice versa.

spherical; and at $\omega_z \ll \omega_\perp$, t he dot is cigar shaped; while the dot becomes planar disk for $\omega_z \gg \omega_\perp$. The transition magnetic field decreases monotonically with the change of geometry from cigar shape through spherical to planar disk. In Fig. 6(b), we show the change of transition magnetic field with respect to the size of vertical quantum dot. In this plot, we set the ratio of $\omega_z : \omega_\perp$ at 5.436. This is to simulate the experimental shape of vertical dot with fixed diameter to height ratio. Since the spatial spreading is $\sim 1/\sqrt{\omega_\perp}$, hence smaller $\omega_\perp$ corresponds to larger dot and larger $\omega_\perp$ means smaller dot. We can see that the transition magnetic field is larger for smaller dots than larger dots. The tendency of change is monotonic, too.

IV. CONCLUSIONS

By using the coupled-channel method, we are able to solve the energy spectra of the two interacting electrons in a vertical quantum dot under magnetic fields. The study takes the vertical dimension into consideration. We find that the *z* confinement has significant effects on the energy spectra. For the quantum dot with larger diameter to height ratio, the magnitude of the magnetic field for the singlet-triplet crossover is larger than the thinner shape quantum dots. And from the difference of total energy between results include and exclude the Coulomb and spin effects, we find that the correlations of the two electrons are more important for low-lying states than the higher one. In the study of correlation energy, effects from quantum dot geometry and the applied magnetic fields were explored. Finally, the method we used in this paper is flexible to other kinds of confinement potentials. We limit the calculation to parabolic confining potential, because the study[10] showed that the model is very accurate. However, in our study of the effects of quantum dot dimensionality and size, the magnitude of the magnetic field for the singlet-triplet crossover is actually dependent on the potential parameters.

ACKNOWLEDGMENTS

The authors acknowledge the National Science Council of Taiwan for financial support under Contract Nos. NSC89-2112-M235-001 and NSC89-2112-M009-044. One of us (J.T.L) was supported by the Computational Materials Research Program, National Center for Theoretical Sciences (NCTS), Taiwan.

[1] M. Wagner, U. Merkt, and A.V. Chaplik, Phys. Rev. B **45**, 1951 (1992).
[2] R.C. Ashoori *et al.*, Phys. Rev. Lett. **71**, 613 (1993).
[3] G.W. Bryant, Phys. Rev. Lett. **59**, 1140 (1987).
[4] U. Merkt, J. Huser, and M. Wagner, Phys. Rev. B **43**, 7320 (1991).
[5] D. Pfannkuche, V. Gudmundsson, and P.A. Maksym, Phys. Rev. B **47**, 2244 (1993).
[6] M. Dineykhan and R.G. Nazmitdinov, Phys. Rev. B **55**, 13 707 (1997); J. Phys.: Condens. Matter **11**, L83 (1999).
[7] C. Sikorski and U. Merkt, Phys. Rev. Lett. **62**, 2164 (1989).
[8] M. Macucci, K. Hess, and G.J. Iafrate, Phys. Rev. B **48**, 17 354 (1993); M. Macucci, K. Hess, and G.J. Iafrate, J. Appl. Phys. **77**, 3267 (1995); G.J. Iafrate, K. Hess, J.B. Krieger, and M. Macucci, Phys. Rev. B **52**, 10 737 (1995); M. Macucci, K. Hess, and G.J. Iafrate, *ibid.* **55**, 4879 (1997).
[9] M. Rontani, F. Rossi, F. Manghi, and E. Molinari, Phys. Rev. B **59**, 10 165 (1999).
[10] N.A. Bruce and P.A. Maksym, Phys. Rev. B **61**, 4718 (2000); A. Aharony, O. Entin-Wohlman, and Y. Imry, *ibid.*, **61**, 5452 (2000); C.E. Creffied, J.H. Jefferson, S. Sarkar, and D.L.J. Tipton, *ibid.*, **62**, 7249 (2000); C. Yannouless and U. Landman, Phys. Rev. Lett. **85**, 1726 (2000).
[11] T.F. Jiang, X.M. Tong, and S.I. Chu, Phys. Rev. B **63**, 045317 (2001).
[12] B.K. Ridley, *Quantum Processes in Semiconductors*, 2nd ed. (Claredon Press, Oxford, 1988).
[13] G. Yao and S.I. Chu, Chem. Phys. Lett. **204**, 381 (1993).
[14] J. Wang, S.I. Chu, and C. Laughlin, Phys. Rev. A **50**, 3208 (1994).